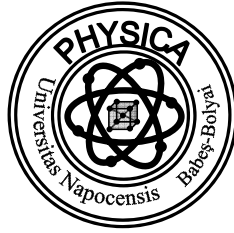


“BABEȘ-BOLYAI” UNIVERSITY
Faculty of Physics



Maria Simona Guțoiu

PhD. Thesis summary

Structural and magnetic properties of hard/soft
exchanged coupled materials

Scientific supervisor
Prof. dr. Viorel Pop

Cluj-Napoca
2011

Thesis content

Introduction	1
---------------------------	----------

Chapter 1 Magnetic materials

1.1. Soft magnetic materials	3
1.2. Hard magnetic materials.....	7
1.3. Exchange coupled magnetic materials	12
1.3.1. SmCo ₅ /Fe, SmCo ₅ /Fe ₆₅ Co ₃₅ type nanocomposite	16
1.3.2. R ₂ Fe ₁₄ B + soft magnetic phase based on Fe type nanocomposite	24

Chapter 2 Techniques and experimental methods

2.1. Experimental techniques for sample preparation	32
2.1.1. Electric arc furnace and induction furnace.....	32
2.1.2. Mechanical dry milling.....	35
2.1.3. Annealing.....	39
2.2. Methods of study.....	40
2.2.1. X-ray diffraction.....	40
2.2.2. Differential scanning calorimetry analysis	43
2.2.3. Scanning electron microscopy (SEM).....	44
2.2.4. Magnetic measurements. Vibrating sample magnetometer and extraction field magnetometers.....	45
2.2.4.1. Vibrating sample magnetometer.....	46
2.2.4.2. Magnetometers with axial extraction of the sample in magnetic field....	47

Chapter 3 Sample preparation

3.1. Preparation of hard magnetic phase, R ₂ Fe ₁₄ B.....	49
3.2. Preparation of soft magnetic phase, α -Fe and hard magnetic phase of Nd ₂ Fe ₁₄ B type.....	50
3.3. Preparation of nanocomposite powders of R ₂ Fe ₁₄ B + x% Fe (x =10, 22) type.....	51
3.4. Annealing applied.....	51

Chapter 4 The influence of milling and annealing conditions on the crystallographic and magnetic properties of soft magnetic phase, Fe and hard magnetic phase, Nd₂Fe₁₄B.

4.1. Structure and microstructure evolution of hard magnetic phase, Nd ₂ Fe ₁₄ B depending on milling and annealing conditions.....	53
4.2. Structure and microstructure evolution of soft magnetic phase, Fe depending on milling and annealing conditions.....	59

4.3.	Study by scanning electron microscopy of microstructure of hard magnetic phase, Nd ₂ Fe ₁₄ B.....	64
4.4.	The evolution of magnetic behaviour of hard magnetic phase, Nd ₂ Fe ₁₄ B.....	66
4.5.	The evolution of magnetic behaviour of soft magnetic phase, Fe.....	72
4.6.	Comparative study of Fe and hard magnetic phase, Nd ₂ Fe ₁₄ B crystallization depending on annealing time.....	74
4.7.	Conclusions.....	76

Chapter 5 The influence of milling and annealing conditions on the crystallographic and magnetic properties of R₂Fe₁₄B + x wt% α-Fe nanocomposite (where x = 10 or 22; R = Nd, Nd+Dy).

5.1.	Structure and microstructure evolution of Nd ₂ Fe ₁₄ B + 10 wt% α-Fe magnetic nanocomposite depending on milling and annealing conditions.....	78
5.2.	Structure and microstructure evolution of R ₂ Fe ₁₄ B + 22 wt% α-Fe (R = Nd, Nd+Dy) magnetic nanocomposite depending on milling and annealing conditions.....	87
5.3.	Study of magnetic behaviour and exchange coupling of Nd ₂ Fe ₁₄ B + 10 wt% α-Fe magnetic nanocomposite.....	93
5.4.	Study of magnetic behaviour and exchange coupling of R ₂ Fe ₁₄ B + 22 wt% α-Fe (R = Nd, Nd+Dy)magnetic nanocomposite.....	103
5.5.	Comparative study of nanocomposite R ₂ Fe ₁₄ B + x wt% α-Fe (where R = Nd, Nd+Dy and x = 10 or 22).....	114
5.6.	Conclusions.....	119

General conclusions and perspectives.....121

References.....123

List of papers.....128

Keywords: magnetic nanocomposite, mechanical milling, hysteresis, rapid annealing, exchange coupled.

Introduction

Along with the evolution of human society the interest in understanding and usage has also increased the interest in various practical applications of natural phenomena such as magnetism and related magnetic behaviour of the substance. Long after their discovery, magnetic phenomena have been studied only on a macroscopic scale and only in the last century atomic-scale magnetic phenomena have been studied and understood. Exchange interaction, crystal field interaction with magnetic moments and relativistic spin-orbit coupling which are atomic-scale magnetic phenomena have been extensively exploited in permanent magnets based on intermetallic compounds of 3d transition metals with rare earth R (magnets Sm-Co or $R_2Fe_{14}B$ type). Achieving high performance magnetic materials, even there is about hard or soft magnetic materials, involves materials with remarkable intrinsic magnetic properties (saturation magnetisation, Curie temperature, anisotropy constant, magnetostriction constant etc.). Nanocrystalline magnetic materials present interesting magnetic properties regarding both fundamental research and applications. They play an important role in the field of hard and soft magnetic materials. Theoretical calculation shows that the preparation of hard/soft magnetic composite with dimensions of crystallites or thin layers at nanometric scale would allow using all the potential of the two classes of magnetic materials: large anisotropy – hard magnetic materials – and higher magnetization – soft magnetic materials. The result is a new class of hard magnetic materials namely hard/soft nanocomposite or spring magnets. The development of obtaining techniques and study methods has led to the discovery and understanding of new phenomena that characterize these materials, as is the exchange coupling.

The promising energy product obtained in the case of nanocomposite magnets based on Nd-Fe-B system, has pointed out these materials as potential candidates for performing hard magnetic materials. This paper proposes the study of $R_2Fe_{14}B + x \text{ wt}\% \alpha\text{-Fe}$ magnetic nanocomposite (where $x = 10$ or 22 , $R = \text{Nd}$, Nd+Dy) and also a study of hard $\text{Nd}_2\text{Fe}_{14}\text{B}$ and soft $\alpha\text{-Fe}$ separately magnetic phases. Samples were obtained by mechanical milling and subsequently annealed. Mechanical milling allows the obtaining of homogeneous powders at nanometric scale. We proposed two types of annealing – conventional heat treatment and short heat treatment. By both modes of heat treatment we have desired to restore the structure of hard magnetic phase without leading to excessive growth of crystallite dimensions of soft phase.

The paper is structured in five chapters, ending with a chapter containing general conclusions and perspectives. In the first chapter of the paper we present the main classes of magnetic materials and each specific property. Within exchange enhanced magnetic materials were presented SmC_5 /soft magnetic phase based on Fe and $R_2Fe_{14}B$ /soft magnetic phase based on Fe.

The second chapter contains a brief overview of the main methods of obtaining the materials studied in this work and the used study methods.

Chapter three presents in detail the methodology to obtain the powders of soft and hard magnetic phases and the powders of $R_2Fe_{14}B/Fe$ magnetic nanocomposite. There are also detailed the technical aspects of the way perform annealing.

Crystallographic properties determined by X-ray diffraction, XRD, microstructure evolution determined by XRD, and scanning electron microscopy and magnetic properties determined by measurement of magnetic hysteresis of hard and soft phases are described in chapter four. In order to determine the optimum annealing conditions were performed differential scanning calorimetry measurements that have described structural and microstructural transformations of the studied sample.

The last chapter of the thesis presents the study of the influence of the structure and microstructure of magnetic nanocomposite materials on the interphase exchange coupling between hard and soft magnetic phase. There were presented the study of structured and magnetic properties of four sets of samples, two different reports between hard and soft phases (10 and 22 wt%) and two different types of annealing (classical and short time annealing)

In the final part of the paper are presented general conclusions and perspectives of research in the field concerned. The main conclusions of the research are highlighted and there are also mentioned the effects of milling and annealing conditions on the evolution of the structure, microstructure and magnetic behaviour of samples. List of articles published in professional journals and/or presented at international or national conferences is presented at the end.

Chapter 1

MAGNETIC MATERIALS

In this chapter are presented the main classes of magnetic materials (soft magnetic materials, hard magnetic materials, exchange enhanced magnetic materials) indicating the specific magnetic properties and their utility in applications.

1.1. Soft magnetic materials

Soft magnetic materials are those materials which can be magnetized and demagnetized easily; presenting small coercitive fields, high permeability and high mobility of magnetic domains walls. For certain applications, soft magnetic materials provide high saturation induction (B_s), high Curie temperature and low electrical conductivity. Soft magnetic phases are characterized by weak magnetocrystalline anisotropy imposed firstly, by the high symmetry crystalline structure.

The main classes of soft magnetic materials are:

- A. Soft magnetic materials based on iron
- B. Iron-nickel and iron-cobalt soft magnetic materials
- C. Soft ferrite
- D. Soft amorphous magnetic materials

1.2. Hard magnetic materials

Hard magnetic materials are characterized by high coercive fields, high remanent magnetization large hysteresis loops. The coercive fields values are between 102 and 106 A/m. Besides high coercivity, the practical use of these materials requires high values of Curie temperature, T_C , remanent induction, B_r , and maximum energy product $(BH)_{max}$.

Magnetic anisotropy is an intrinsic factor which leads to large coercivity materials. Depending on the type of anisotropy two types of permanent magnets are obtained. The first category is based on the anisotropy given by the shape of the particles and includes AlNiCo and steel type permanent magnets. The second category is based on nanocrystalline anisotropy and includes hard ferrite permanent magnets and permanent magnets based on rare earth.

The development of techniques for obtaining pure rare earth and the development of melting methods in vacuum or inert gas led to the investigation of a new type of alloys *based on rare earth and 3d transition metals*. Transition metals such as: Mn, Fe, Co, Ni and Cu are

used as alloying elements with rare earth. Since 1983 [6] has been developed a new class of iron – based permanent magnets, $R_2Fe_{14}B$. These magnets can be obtained in both crystalline and amorphous state. An important advantage of Fe – based magnets is the low production cost. The magnetic behavior of $R_2Fe_{14}B$ type magnets is shown in a parallel coupling between magnetic moments of iron and magnetic moments of light rare earth and also an antiparallel coupling between iron and heavy rare earth moments.

1.3 Exchange coupled magnetic materials

At the beginning of 1991, Kneller et al. [11] showed that a mixture of hard ($Nd_2Fe_{14}B$) and soft (Fe_3B/α -Fe) magnetic nanogreins, coupled by exchange interactions can lead to a maximum energy product $(BH)_{max}$ of 200 kJ/m^3 , increasing the interest to study those compounds. Understanding the concept of “exchange coupling” [11] lead to new ways of obtaining high performant hard magnetic materials. Combining the high coercivity of hard magnetic phase with high magnetization of soft magnetic phase can lead to a new class of materials with high value of the energy product. Beside an important energy product it is desired to consider the increase in thermal stability by high Curie temperature, which ensure a stable functionality at the used temperature and an improved corrosion resistance, especially of high importance for the magnets used in a hot and wet climate. The microstructural change of the material must be also considered.

The materials obtained by a coupling between hard and soft nanocrystalline phases are known as exchange coupling magnets or spring magnets [11,12,13-19]. In the soft/hard exchange coupled magnets the coercivity of soft magnetic is realized on interphase exchange interaction with hard magnetic phase, strongly anisotropic. Exchange coupling could generate an energy product up to 795 kJ/m^3 [20], which is much higher than maximum value of the specific energy product $(BH)_{max}$, obtained for the actual magnets on the market. The calculation made by Skomski [106] on $Sm_2Fe_{17}N_3/Fe_{65}Co_{35}$ nanocomposite type magnets show the possibility of obtaining 1090 kJ/m^3 specific energies.

Due to unconventional methods of preparation, hard to replicate on industrial level, hard nanocomposite materials have no direct interest and their economic impact has proven to be partially neglected for a long time. With the development of preparation techniques increasing magnetic performance of magnetic materials and also with increasing of marked requirements we see a growing interest of the magnetic materials producers new production technologies and implementation of these materials. As regards the applications, the most important parameter for permanent magnet is represented by $(BH)_{max}$.

Alloying/mechanical milling was intensive used for preparation of metastable phases with various interesting magnetic properties, including intensive exchange coupling [41-50].

In these systems have been reported relatively large magnetic properties of 326 kJ/m^3 [36]. The influence of annealing and mechanical milling on structure and magnetic behaviour of magnetic nanocomposite based on Fe (soft magnetic phase) and hard phases on intermetallic compounds with rare earth highlights the importance of *structure and microstructure* on *strength of exchange coupling* between hard and soft magnetic phases [33, 51-55]

Chapter 2

TECHNIQUES AND EXPERIMENTAL METHODS

The chapter contains a brief overview of preparation techniques and annealing used to obtain the studied $\text{R}_2\text{Fe}_{14}\text{B}/\alpha\text{-Fe}$ nanocomposite. The methods of structural and magnetic investigation are also presented.

Chapter 3

SAMPLE PREPARATION

3.1. Preparation of hard magnetic phase, $\text{R}_2\text{Fe}_{14}\text{B}$

In order to obtain the hard magnetic phases were used chemical elements with 99.9 % purity. Calculations were made for the desired composite, taking into account the proportions of materials components.

Due to the reactivity of oxygen with rare earth, the alloys were prepared by arc furnace under argon atmosphere. To ensure that the working atmosphere is clean, we have evacuated several times the chamber and each time was filled with argon. Before the melting of the sample we melted a piece of titanium (at high temperatures titanium catch the oxygen) in order to clean oxygen impurities of the chamber. For sample preparation we have repeated the melting to ensure an adequate homogenization. In some cases we have made use of an induction oven for a better homogenization.

In order to obtain a structural homogenization the sample were annealed for a long time under high vacuum of 10^{-6} mbar. The annealed temperature was 1223 K, and the annealing time was 72 hours.

3.2. Preparation of soft magnetic phase, α -Fe and hard magnetic phase of $\text{Nd}_2\text{Fe}_{14}\text{B}$ type.

Soft, α -Fe and hard, $\text{Nd}_2\text{Fe}_{14}\text{B}$ magnetic powders were obtained by mechanical milling using a planetary mill, Frish Pulverisette 4 type, with two vials that allow working in controlled atmosphere. Rotation of the vials is in opposite direction with the platform. The following milling condition were used, speed of the vials: $\omega = -900$ rpm; speed of the platform $\Omega = 333$ rpm..

The milling was performed in heat – treated steel vial with a volume of 80 ml. A vial was used for mechanical milling of soft magnetic phase of commercial iron powder 100.24CN, having a particle size under 40 μm . The second vial was used to obtain the hard magnetic phase, $\text{Nd}_2\text{Fe}_{14}\text{B}$ powders. With Fe respectively $\text{Nd}_2\text{Fe}_{14}\text{B}$ magnetic powders, were put 15 grinding balls in each vial, the ratio between the mass of magnetic materials and the mass of grinding ball is 10:1. The vials were sealed in an oxygen – free inert environment (argon gas) inside a glove box.

The milling was performed for 12 hours, taking test sample at 1, 2, 4, 6, 8 and 12 hours, each test sample having a mass of about 0.5 g. The powders obtained were annealed at 500, 550, 600 $^\circ\text{C}$ – conventional annealing and respectively at 800 $^\circ\text{C}$ – short time annealing.

3.3. Preparation of nanocomposite powders of $\text{R}_2\text{Fe}_{14}\text{B} + x\%$ Fe ($x = 10, 22$) type.

In order to obtain composite magnetic sample the hard magnetic phase $\text{R}_2\text{Fe}_{14}\text{B}$ was co – milled with soft magnetic phase α – Fe. After preliminary milling for 2 hours of hard phase was added the powder of soft magnetic phase α – Fe in 10 and 22 weight percent. The powder size of the iron was under 40 μm . The milling was performed for 4, 6, 8 and 12 hours. The ball – to – powder ratio was 1:10. Technical conditions of milling were identical to those used for milling soft and hard phases separately.

3.4. Annealing applied

The first annealing technique – classical heat treatment or long time heat treatment – consist in heating the samples at temperature of 500 – 600 $^\circ\text{C}$ for 1,5 hours to 14 hours and at

800 °C for 5 minutes. In the paper we use the notation HT referring to heat treatment and CHT referring to conventional heat treatment.

The second heat treatment technique - short heat treatment – is a new method of heating the samples. By this method we try to study the influence of annealing conditions on crystallographic and magnetic properties of milled samples. Annealing was performed at temperatures between 700 and 800 °C. The annealing was done for short durations at times between 0.5 and 3 minutes. In the paper we use the notation SHT referring to short time heat treatment.

Chapter 4

THE INFLUENCE OF MILLING AND ANNEALING CONDITIONS ON THE CRYSTALLOGRAPHIC AND AMGNETIC PROPERTIES OF SOFT MAGNETIC PHASE, Fe AND HARD MAGNETIC PHASE, Nd₂Fe₁₄B.

Our previous studies [33, 54, 95, 96] on R₂Fe₁₄B/ α -Fe nanocomposite type show a weak exchange coupling between soft and hard magnetic phases. One of the reasons for this behaviour could be the poor crystallinity of hard magnetic phase and an excessive growth of soft magnetic phase, above the conditions of achieving the exchange coupling between the phases. A solution must be found in order to determine the optimal conditions of annealing. The purpose of these conditions is to restore the crystallinity of hard magnetic phase without leading to a higher growth of crystallites of soft magnetic phase. In order to find appropriate annealing and milling conditions, an individual structural, microstructural and magnetic study of the hard and respectively soft magnetic phase is proposed [97]

4.1. Structure and microstructure evolution of hard magnetic phase, Nd₂Fe₁₄B depending on milling and annealing conditions

The section shows the influence of milling and annealing process on the crystallographic and magnetic properties of hard magnetic phase, Nd₂Fe₁₄B. The structural

evolution from the milling process is shown in figure 4.1. In the figure, which presents diffraction patterns of the sample, we can see that the diffraction peaks increase with increasing milling time and become undetectable at high milling times. This evolution can be attributed to several effects that are induced by milling: the occurrence of induced internal stresses, a decrease of the crystallite size and the amorphisation of the hard phase structure by milling. The presence of the iron diffraction peaks can be attributed to a small quantity of unreacted iron and to the contamination from vials and balls.

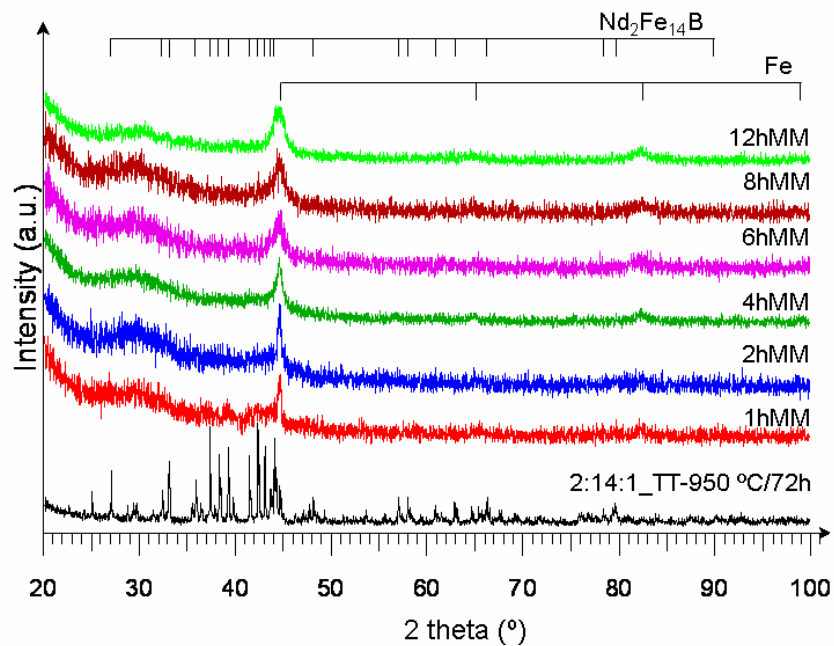


Figure 4.1. X-ray diffraction patterns of Nd₂Fe₁₄B milled from 1 to 12 h, obtained with a diffractometer with Cu K α radiation. The diffraction pattern of Nd₂Fe₁₄B ingot annealed at 950 °C for 72 h is also given for comparison.

In order to optimize the annealing conditions, we have proceeded to some thermal analyses. Figure 4.2 shows DSC (differential scanning calorimetry) curves of Nd₂Fe₁₄B sample milled for 6 h. In the heating process, the exothermic peak above 200 °C, indicates a release of the milling induced internal stress. Around the temperature of 500 °C is reported the presence of exothermic peak corresponding to recrystallization process of iron and Fe₃B phase, while around the temperature of 700 °C the exothermic peak that begins to appear can be attributed to the crystallization of Nd₂Fe₁₄B magnetic phase. In the cooling process, the DSC signal vs. temperature shows only one transformation before 300 °C which is attributed to the Curie temperature, T_C, of Nd₂Fe₁₄B hard phase.

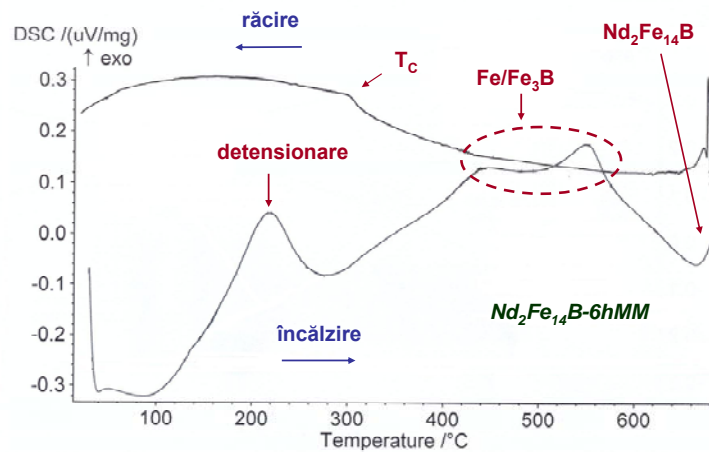


Figure 4.2. measurements of $\text{Nd}_2\text{Fe}_{14}\text{B}$ milled for 6 h.

Based on the analysis of DSC curves, we decided to perform two types of HT: a) classical heat treatment, CHT, made at 500 – 600 °C for 2 h and b) short heat treatment, SHT, made between 700 – 800 °C for 0.5 – 3 minutes.

The structural evolution of hard magnetic phase milled for 12h and annealed at 500, 550, 600 °C for 2 h is presented in diffraction patterns from figure 4.3. The diffraction pattern of pure $\text{Nd}_2\text{Fe}_{14}\text{B}$ ingot annealed at 950 °C for 72 h is also given to be compared.

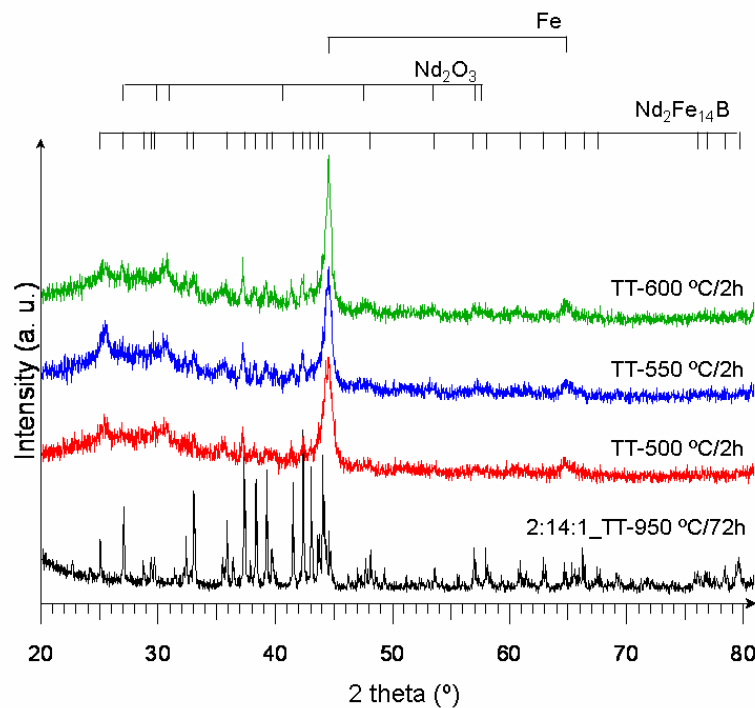


Figure 4.3. X-ray diffraction patterns of $\text{Nd}_2\text{Fe}_{14}\text{B}$ milled for 12 h and classical annealed at indicated temperatures and times. The diffraction pattern of $\text{Nd}_2\text{Fe}_{14}\text{B}$ ingot annealed at 950 °C for 72 h is also given to be compared. The diffractometer use a $\text{Cu K}\alpha$ radiation

While increasing the annealed temperature it can be observed an increase of crystallinity of hard magnetic phase; the corresponding peaks are well resolved and rather thinner.

The diffraction patterns of the sample annealed at 800 °C for 0.5; 1 and 1.5 minutes are shown in figure 4.4. The diffraction pattern of pure Nd₂Fe₁₄B ingot annealed at 950 °C for 72 h is also given to be compared. It is worthy of note that the annealing for 0.5 minutes did not lead to a recovery of crystallinity of hard magnetic phase, the corresponding peaks being undetectable. The best resolved and rather thinner diffraction peaks corresponding to the hard magnetic phase occur for the sample annealed for 1.5 minutes, proving a good crystallinity and a beginning of iron recrystallization.

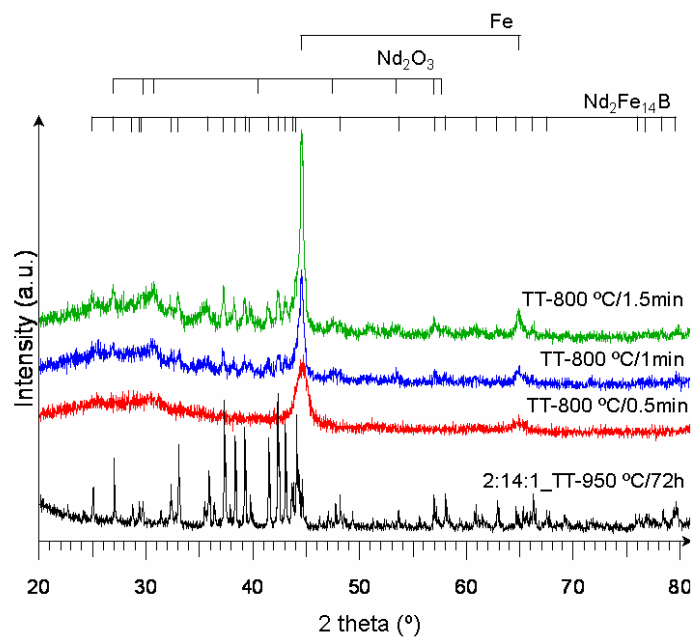


Figure 4.4. X-ray diffraction patterns of Nd₂Fe₁₄B milled for 12 h and short time heat treatment at indicated temperatures and times. The diffraction pattern of Nd₂Fe₁₄B ingot annealed at 950 °C for 72 h is also given to be compared. The diffractometer use a Cu K α radiation

4.2. Structure and microstructure evolution of soft magnetic phase, Fe depending on milling and annealing conditions

The section presents the structural and microstructural evolution of soft magnetic phase obtained by mechanical milling and annealing. The induced milling effects on soft magnetic phase are similar to those induced after milling hard magnetic phase. The annealing lead to rearrangements of atoms in the body centered cubic structure of α -Fe and some recrystallization effects. The nanocrystallites mean size of α -Fe crystallites calculated from

diffraction peak $2\theta = 106^\circ$ ($d = 1.434 \text{ \AA}$), according to Scherrer formula (equation 4.1) [94], Cr radiation, are presented in table 4.1. Scherrer formula is:

$$\beta = \frac{K\lambda}{D \cdot \cos\theta} \quad (4.1)$$

where β is the width of diffraction peak, θ is Bragg angle and λ is the wavelength of X-ray radiation

Table 4.1 Crystallites mean size of α -Fe milled for 12 h and annealed at different temperatures for 2 h, the crystallite size has been calculated according to Scherrer formula

Annealing temperature (°C)	Annealing time (h)	FWHM (°)	D (nm)
500	2	1,27	19 (± 2)
550	2	1,25	19 (± 2)
600	2	1,15	31 (± 2)

Increasing the annealing temperature from 500 to 550 °C does not lead to a significant increase of crystallite size. Instead the annealed performed at 600 °C lead to a net increase of crystallites size value of about 31nm. The evolution of the crystallite size is due to the fact that the temperature values of 500 and 550 °C are close or under close to the temperature of recrystallisation process of Fe, while the temperature of 600 °C is above the recrystallization temperature of Fe, figure 4.2.

The X-ray diffraction patterns of α -Fe samples milled for 12 h and annealed at 800 °C for times between 0.5 and 2 minutes are shown in figure 4.5. For comparison is presented the

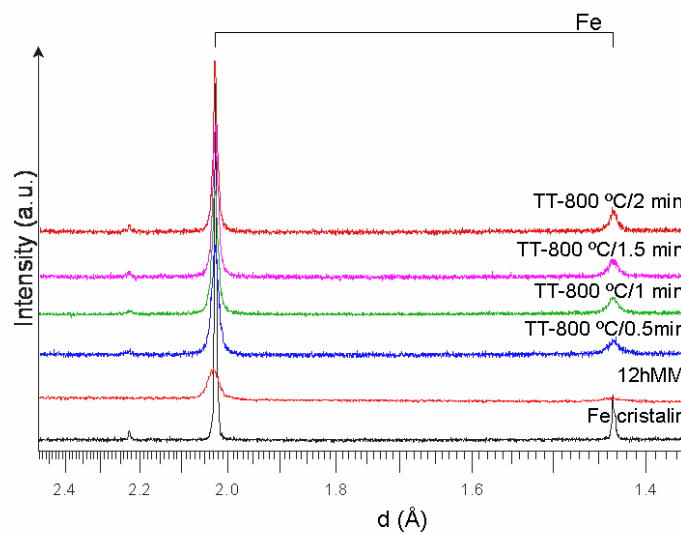


Figure 4.5. X-ray diffraction patterns for 12 h milled Fe samples and annealed at 800 °C for times between 0.5 and 2 minutes. For comparison is shown the starting Fe powder.

diffraction pattern of Fe starting powder (the diffractometer used Cr $K\alpha$ radiation) and 12 h milled sample (the diffractometer used Cu $K\alpha$ radiation). The nanocrystallites mean size of α -Fe crystallites calculated from diffraction peak $2\theta = 106^\circ$ ($d = 1.434 \text{ \AA}$), according to Scherrer formula (equation 4.1) [94], Cr radiation, are presented in table 4.2. The crystallite size is larger for samples annealed at 800 °C compared to samples annealed at 500 or 550 °C. By increasing the annealing time from 1.5 to 2 minutes we obtained crystallites with double size.

Table 4.2. Crystallites mean size of 12 h milled Fe annealed at 800 °C for different times, according to Scherrer formula

Annealing temperature(°C)	Annealing time (min)	FWHM (°)	D (nm)
800	1,0	1,13	22 (± 2)
	1,5	1,01	25 (± 2)
	2,0	0,64	49 (± 2)

4.4. The evolution of magnetic behaviour of hard magnetic phase, $\text{Nd}_2\text{Fe}_{14}\text{B}$

The magnetic measurements results are in agreement with structural and microstructural results obtained by X-ray diffraction measurements. The magnetic hysteresis loops for $\text{Nd}_2\text{Fe}_{14}\text{B}$ 12 h milled sample and annealed at 800 °C for times between 0.5 and

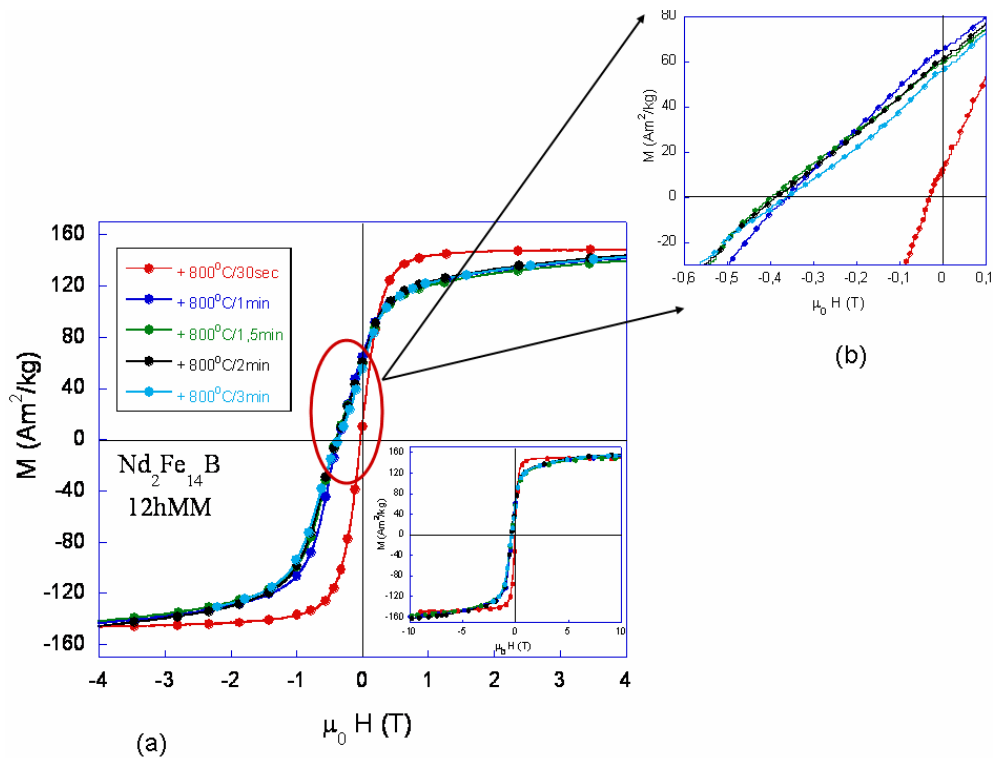


Figure 4.6. Hysteresis loops recorded for $\text{Nd}_2\text{Fe}_{14}\text{B}$ samples milled for 12h and annealed at 800 °C for the indicated time (a) hysteresis loops for the same samples presented in selected region (b)

3 minutes are shown in figure 4.6. By performing HT, there is an increase of coercivity from 0.03 to 0.40 T. Increasing annealing time lead to a higher coercivity. The magnetization of the samples annealed between 1 and 3 minutes dose not reach the saturation in field of 10 T indicated a strong increase in anisotropy by recovering the crystalline structure of hard magnetic phase, $\text{Nd}_2\text{Fe}_{14}\text{B}$ after HT. The magnetization of the sample annealed for 0.5 minutes at 800 °C reach the saturation faster indicating a poor crystallinity of hard phase after milling and annealing, the results being in agreement with structural data discussed above.

The evolution of the coercivity of the samples depending on the annealing time for SHT is shown in figure 4.7. There is a sudden increase in the value of coercivity from 0.03 T for sample annealed for 0.5 minutes at 800 °C to a value of 0.36 T for the sample annealed for 1 minute at 800 °. This result is in agreement with XRD results, where we find a high crystallisation of the sample after 1 minute of HT and a net increase of crystallite size with increasing annealing time, figure 4.5 and table 4.2. The coercivity has a maximum for the sample annealed for 1.5 minutes and after that the coercivity has a slight decrease to a value of 0.36 T for the sample treated for 3 minutes. This evolution may be caused by a poor exchange coupling between hard and traces of the soft magnetic phases of the samples. Also, at higher annealing times, higher than 1.5 minutes there is a reduction of defects (significant center for peening for domain wall) induced by milling which lead to lower coercivity.

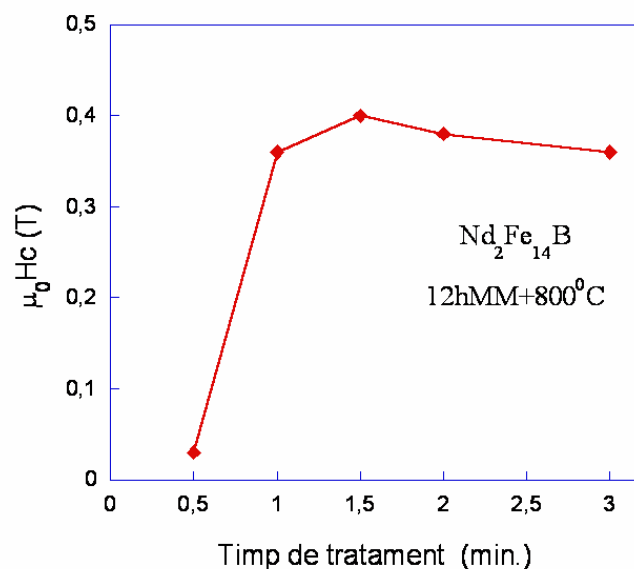


Figure 4.7 The coercivity of $\text{Nd}_2\text{Fe}_{14}\text{B}$ samples milled for 12 h and annealed at 800 °C depending on annealing time.

4.7. Conclusions.

In this chapter we presented the structural and magnetic results of hard, Nd₂Fe₁₄B and soft, Fe magnetic phases. The study and interpretation of magnetic properties was carried out in direct correlation with the results of structural and microstructural studies. These researches have the final goal use hard and soft magnetic phases in exchange coupled nanocomposite. The main results of the study could be summarized as follows:

- With increasing milling time one can notice a progressive crystallinity destruction of phases. This behavior is much obvious for hard magnetic phase, Nd₂Fe₂B.
- Differential scanning calorimetry allowed the determination of annealing conditions, which lead to the restoration of the crystallinity of hard magnetic phase, without a net increasing of crystallites of soft magnetic phase. We consider that solving this problem consists of a triple correlation between the times of milling time of annealing and temperature of annealing.
- We performed two types of annealing: classical heat treatment (CHT) at annealing times of 1-2 hours, and short time heat treatment (SHT) at times of annealing up to 3 minutes. The first of these was done around the recrystallization temperature of iron; the second was carried out at temperatures higher than the recrystallization temperature of the hard phase.
- The optimum annealing temperature for CHT is around 550 °
- The best condition of annealing for SHT was determined to be around 800 °C temperature for 1 minute time.
- The crystallite main size for Fe, according to Sherrer formula was around 20 nm for both HT.
- Comparing the degree of crystallinity of the hard magnetic phase annealed by the two methods we concluded that SHT provide a better crystallization of this phase, keeping an optimum size of Fe crystallites.
- For the CHT the essential parameter in crystallinity restoration of hard magnetic phase is the temperature while for SHT not only temperature but also the time plays an important role in achieving optimal structure and microstructure of the two phases. Annealing time is a critical parameter for SHT, while for the CHT for 2 hours of annealing no significant changes occur in crystallographic evolution of the samples.

Chapter 5

THE INFLUENCE OF MILLING AND ANNEALING CONDITIONS ON THE CRYSTALLOGRAPHIC AND MAGNETIC PROPERTIES OF $R_2Fe_{14}B + x$ wt % α -Fe NANOCOMPOSITE (WHERE $x = 10$ OR 22 , $R = Nd, Nd+Dy$)

The study of structure and microstructure of $R_2Fe_{14}B + x$ wt % α -Fe magnetic nanocomposit (where $x = 10$ or 22 , $R = Nd, Nd+Dy$) has considered the influence of preparation conditions (milling and annealing) on interphase exchange coupling between hard and soft magnetic phase. In this chapter we present the study of structural and magnetic properties of four sets of sample, two different proportions between hard and soft phases and two types of annealing conditions.

- a) Samples obtained by mechanical milling between 2 and 12 h, followed by long heat treatment
 1. $Nd_2Fe_{14}B + 10$ % wt α -Fe
 2. $(Nd_{0.92}Dy_{0.08})_2Fe_{14}B + 22$ % wt α -Fe
- b) Samples obtained by mechanical milling for 8 h, followed by short time heat treatment
 3. $Nd_2Fe_{14}B + 10$ % wt α -Fe
 4. $Nd_2Fe_{14}B + 22$ % wt α -Fe

Studying the calorimetric curves we proposed the tow types of annealing conditions that were studied. Because for all the samples we worked with weight % of Fe, to simplify the notation, %Fe must be understood as meaning the refers to the percentage of weight of iron.

5.1. Structure and microstructure evolution of $Nd_2Fe_{14}B + 10$ wt% α -Fe magnetic nanocomposite depending on milling and annealing conditions.

Structural study of $Nd_2Fe_{14}B + 10\%$ α -Fe nanocomposite [96, 104, 107] obtained by mechanical milling were performed by X-ray diffraction measurements. Figure 5.1. shows the diffraction patterns of 4 to 12 hour milled samples. The evolution of milled magnetic nanocomposite samples is similar with the evolution of hard magnetic phase described in

chapter 4. From the diffraction patterns we can observe that for long milling times the corresponding diffraction peaks of hard magnetic phase become undetectable. This evolution can be explained by appearance of several effects: amorphisation of hard magnetic phase by milling, a decrease of crystallite size the occurrence of induced internal stress and defects. The width of diffraction peak increase for long milling times, but they are still detectable in comparison with peaks of hard magnetic phase.

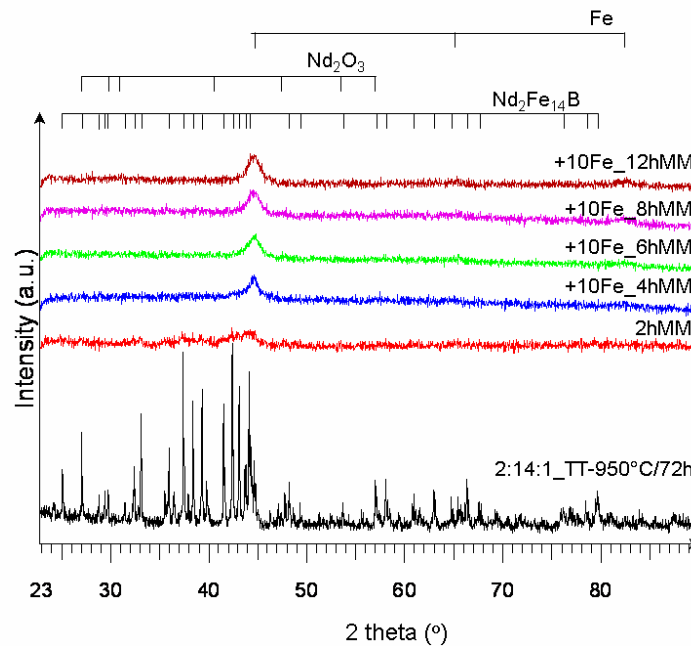


Figure 5.1. X-ray diffraction patterns of the $\text{Nd}_2\text{Fe}_{14}\text{B}+10\% \alpha\text{-Fe}$ milled between 4 and 12 h. The diffraction pattern of $\text{Nd}_2\text{Fe}_{14}\text{B}$ ingot annealed at 950 °C for 72 h and the diffraction pattern of $\text{Nd}_2\text{Fe}_{14}\text{B}$ milled for 2 h are also given for comparison. The diffractometer used a $\text{Cu } K\alpha$ radiation.

As was mentioned in chapter 4, the optimum annealing temperature for CHT was 550 °C; at this temperature we succeeded to restore the crystallinity of hard magnetic phase, $\text{Nd}_2\text{Fe}_{14}\text{B}$ without an excessive growth of soft magnetic phase. Considering these results the CHT has been performed at 550 °C for 1.5 h. The HT led to improvement of crystallinity of the sample as it was shown in figure 5.2. Compared to the only milled samples the annealed samples present a recovery of the diffraction peak corresponding to the hard magnetic phase and a rather thinner peak corresponding to the soft magnetic phase. While increasing the milling time the refinement of the structure of hard magnetic phase, $\text{Nd}_2\text{Fe}_{14}\text{B}$ become more difficult. Due to release of the internal stress at temperatures between 200 and 300 °C [98] we can neglect their contribution to the width of diffraction sample annealed at 550 °C.

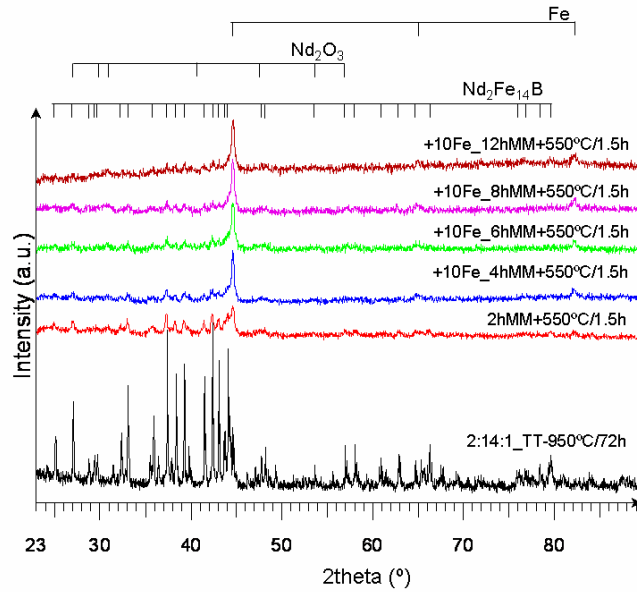


Figure 5.2. X-ray diffraction patterns for $\text{Nd}_2\text{Fe}_{14}\text{B}+10\% \alpha\text{-Fe}$ samples milled between 4 and 12 h and annealed at 550 °C for 1.5 h. The diffraction pattern of $\text{Nd}_2\text{Fe}_{14}\text{B}$ ingot annealed at 950 °C for 72 h and the diffraction pattern of $\text{Nd}_2\text{Fe}_{14}\text{B}$ milled for 2 h and annealed at 550 °C for 1.5h are also given for comparison. The diffractometer used a $\text{Cu } K\alpha$ radiation.

The diffraction patterns of $\text{Nd}_2\text{Fe}_{14}\text{B}+10\% \alpha\text{-Fe}$ nanocomposite samples milled 8 h and annealed at 700 and 800 °C for a period of time between 1 and 2 minutes are shown in figure 5.3. In most cases the diffraction patterns show well resolved peaks corresponding to

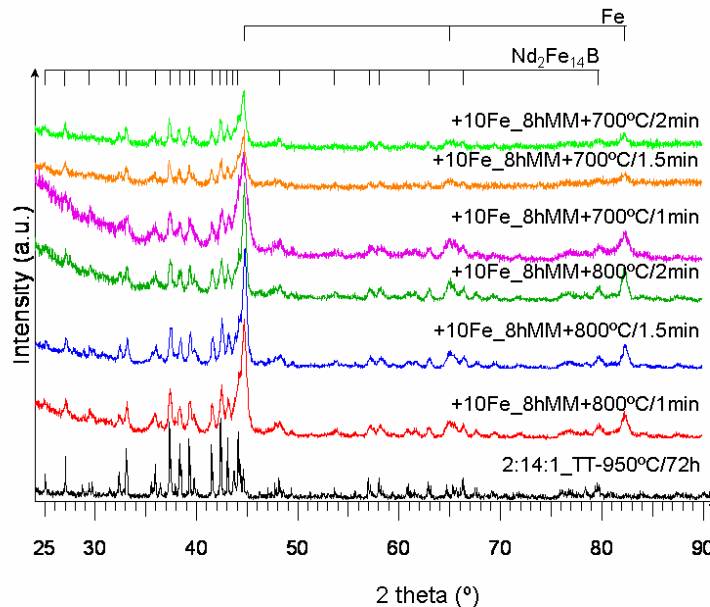


Figure 5.3. X-ray diffraction patterns of 8 hours milled nanocomposite and annealed at temperatures of 700 and 800 °C for times between 1 and 2 minutes. The diffraction pattern of $\text{Nd}_2\text{Fe}_{14}\text{B}$ ingot annealed at 950 °C for 72 h is given for comparison. The diffractometer used a $\text{Cu } K\alpha$ radiation.

the hard magnetic phase. This evolution indicates a good crystallinity of the samples annealed at temperatures between 700 and 800 °C. The characteristic diffraction peaks of α -Fe phase are large proving that HT dose not lead to an excessive size growth of soft magnetic phase. Comparison with the peaks of Nd₂Fe₁₄B ingot, the composite samples milled for 8 h and rapidly annealed at 700 and 800 °C present broader peaks, proving the small crystallites obtained after milling and annealing. The additional diffraction peaks after HT are not observed additional in diffractions.

The crystallites mean sizes of α -Fe phase in a Nd₂Fe₁₄B/ α -Fe nanocomposite milled for 8 hours and annealed, calculated from diffraction peak $2\theta = 82.33^\circ$ according to Scherrer formula (see 4.1. equation) are given in table 5.1. For both cases of annealed samples, classical

Table 5.1. The crystallites mean size of α -Fe phase in a Nd₂Fe₁₄B + 10% α -Fe composite milled for 8 h and annealed at different temperatures and times. The crystallite size has been calculated according to Scherrer's formula from XRD patterns obtained with Cu $K\alpha$ radiation.

Annealing temperature (°C)	Annealing time (minute)	FWHM (°)	D (nm)
800	1,0	0.61	17 (± 2)
	1.5	0.50	21 (± 2)
	2,0	0.43	25 (± 2)
700	1,0	0.88	12 (± 2)
	1.5	0.77	14 (± 2)
	2,0	0.66	16 (± 2)
550	90	0.40	26 (± 2)

and rapid annealing, we believe that the internal stresses were removed due to the temperatures that caused them; consequently, their contribution to the FWHM was neglected. For all rapid heat treatment up to 2 minutes the crystallites are smaller than 25 nm. The small size of the crystallites obtained for a sample annealed at 700 °C for 1 minute: 12 nm, entitles us to believe that no significant recrystallisation took place during these annealing. Moreover, even in the case of SHT realized at 800 °C for 1 minute, the sizes of Fe crystallites were sufficiently small to expect a good magnetic coupling with hard magnetic phase. It is important to note that the size of Fe crystallites in samples annealed at 550 °C for 1.5 h are 26 nm, being bigger than the Fe crystallites obtained after rapid annealing at higher temperature.

5.2. Structure and microstructure evolution of $R_2Fe_{14}B + 22 \text{ wt}\% \alpha\text{-Fe}$ ($R = \text{Nd, Nd+Dy}$) magnetic nanocomposite depending on milling and annealing conditions.

Our previous studies on Nd-Fe-B/ α -Fe nanocomposite [33, 96, 104, 107] used 22 wt% α -Fe as soft magnetic phase and in the composition of hard magnetic phase Nd was partially substituted with Dy. The structural behaviour of $(\text{Nd}_{0.92}\text{Dy}_{0.08})_2\text{Fe}_{14}\text{B} + 22\% \alpha\text{-Fe}$ magnetic nanocomposite milled between 4 and 12 h is similar with the structural behaviour of $\text{Nd}_2\text{Fe}_{14}\text{B} + 10\% \alpha\text{-Fe}$ magnetic nanocomposite milled up to 12 h (see section 5.1.)

Using the two ways of HT (short heat treatments and long heat treatments) we intend to recover the crystal structure of hard magnetic phase, decrease the density of defects and reduce internal stress by local diffusions. For SHT, where the temperature of annealing is higher than the recrystallization temperature of the two phases some recrystallizations process could be possible. The first sets of the studied samples were annealed for long times, the annealing leading to the effects mentioned above. As a consequence the diffraction peaks of both phases are easily detectable for samples annealed at temperatures above 500-550 °C (figure 5.4.)

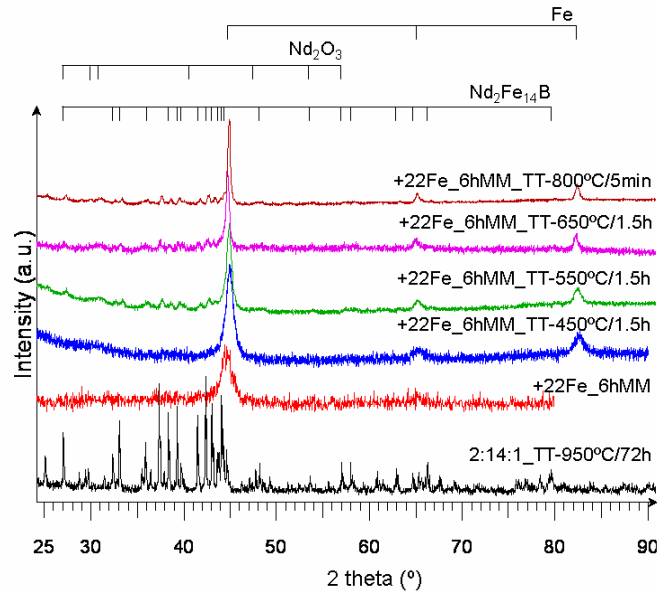


Figure 5.4. X-ray diffraction patterns of $(\text{Nd}_{0.92}\text{Dy}_{0.08})_2\text{Fe}_{14}\text{B} + 22 \text{ wt}\% \alpha\text{-Fe}$ nanocomposite samples milled for 6 h and annealed at indicated temperatures and times in comparison with as milled sample. The diffraction pattern of $\text{Nd}_2\text{Fe}_{14}\text{B}$ ingot annealed at 950 °C for 72 h is also given for comparison. The diffractometer used a $\text{Cu } K\alpha$ radiation.

The second set of studied samples was obtained by 8 h co-milling of 78 wt% hard magnetic phase, $\text{Nd}_2\text{Fe}_{14}\text{B}$ with 22 wt% of soft magnetic phase, $\alpha\text{-Fe}$. After obtaining samples

these were annealed at high temperatures (between 700 and 800 °C) for short time (0.5 to 2.5 minutes). Figure 5.5 presents the diffraction patterns of $\text{Nd}_2\text{Fe}_{14}\text{B}/22\% \alpha\text{-Fe}$ magnetic nanocomposite milled for 8 hours and annealed at temperatures of 700 and 800 °C for times between 1 and 2 minutes. The crystallinity of hard magnetic phase increases while increasing the annealing time. Comparing the sample annealed for 1 minute at 700 °C with the sample annealed for 2 minute at the same temperature we observed a net refinement of the diffraction peaks. Regarding the comparison between the samples annealed at 700 °C and the samples annealed at 800 °C one can see, as we aspect, an increases of the degree of crystallinity of hard magnetic phase once the annealing temperature increases. The characteristic diffraction peaks of soft magnetic phase have an identical evolution with the characteristics diffraction peak of hard magnetic phase. Through this way of annealing the high temperature of heat treatment can lead to the reducing of the defects and the rearrangements of atoms in crystal structure and also lead to possible recrystallisations effects.

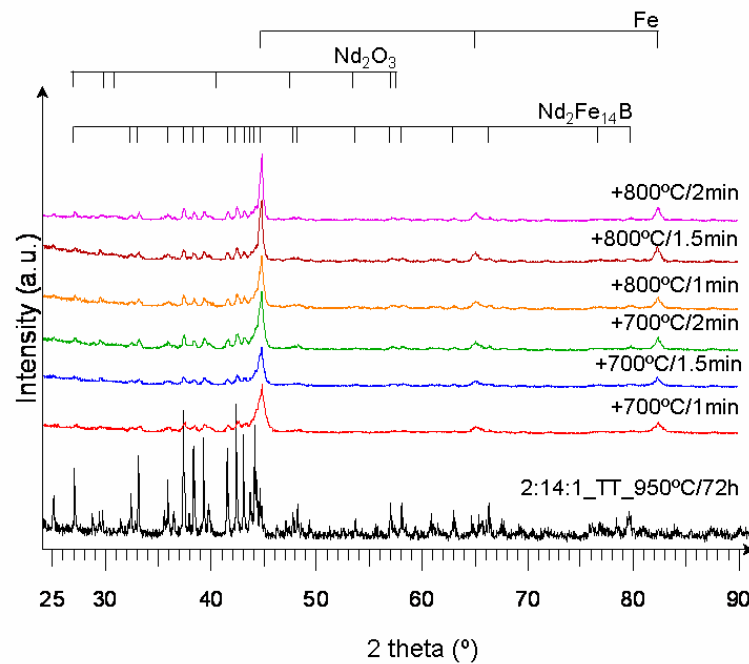


Figure 5.5. X-ray diffraction patterns of $\text{Nd}_2\text{Fe}_{14}\text{B} + 22\% \text{Fe}$ magnetic nanocomposite milled for 8 h and annealed at indicated time and temperature. The diffraction pattern of $\text{Nd}_2\text{Fe}_{14}\text{B}$ ingot annealed at 950 °C for 72 h is also given for comparison. The diffractometer used a $\text{Cu } K\alpha$ radiation.

In order to find the optimal conditions to achieve the exchange coupling between hard and soft magnetic phases the crystallites mean size of soft phase in an $\text{Nd}_2\text{Fe}_{14}\text{B}/22\% \alpha\text{-Fe}$ magnetic nanocomposite have been calculated. The crystallite mean dimensions were calculated using Sherrer's formula (equation 4.1) from the diffraction peak at about 82°. Table

5.2 presents the mean size of α -Fe in Nd₂Fe₁₄B/22% α -Fe magnetic nanocomposite annealed at 700, 750 and 800 °C for times between 1 and 2 minutes. Studing the results of crystallite size dimensions and taking into account the magnetic measurement results (section 5.4.) we can find that the optimum annealing conditions for obtaining a maximum exchange coupling between hard and soft magnetic phases. These condition are realized at annealing temperature of 700, 750 and 800 °C for times of 2, 1.5 and respectively 1 minute.

Table 5.2. The crystallite mean size of α -Fe phase in a Nd₂Fe₁₄B + 22 % α -Fe composite milled for 8 h and annealed at indicated time and temperature. The crystalite size has been calculated according to Scherrer's formula from XRD patterns obtained with Cu K α radiation.

Temperatura de tratament termic (°C)	Timpul de tratament termic (minute)	FWHM (°)	D (nm)
700	1,0	0,82	15 (\pm 2)
	1,5	0,58	19 (\pm 2)
	2,0	0,48	24 (\pm 2)
750	1,0	0,68	19 (\pm 2)
	1,5	0,61	22 (\pm 2)
	2,0	0,50	28 (\pm 2)
800	1,0	0,56	24 (\pm 2)
	1,5	0,53	27 (\pm 2)
	2,0	0,48	30 (\pm 2)

5.3. Study of magnetic behaviour and exchange coupling of Nd₂Fe₁₄B + 10 wt% α -Fe magnetic nanocomposite

The magnetic measurements for studing the Nd₂Fe₁₄B + 10 % Fe magnetic nanocomosite [96,104, 107] were performed by vibrating sample magnetometer in magnetic field up to 10 T at room temperature 300 K. The results of magnetic measurements of milled composites and milled and annealed composites are in agreement with structural and microstructural measurement results.

The magnetic hysteresis loops of Nd₂Fe₁₄B+10 % Fe samples milled between 4 and 12 h and HT at 550 °C for 1.5 h and magnetic hysteresis loops of hard magnetic phase milled for 2 h and annealed in the same conditions were shown in figure 5.6.

The performed annealing leads to improved magnetic properties the coercivity reaching the value of 0.58 T for the sample milled for 4 h. For sample milled for long milling times (12 hours) the annealing does not lead to an improving of coercivity equally to the

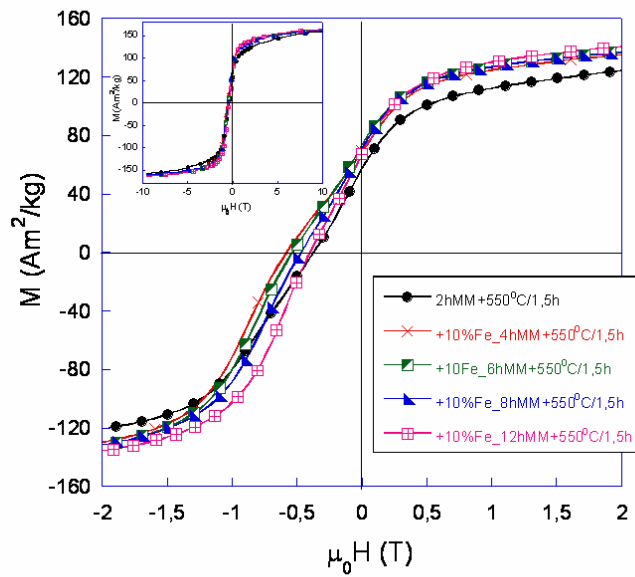


Figure 5.6. Magnetic hysteresis loops of $\text{Nd}_2\text{Fe}_{14}\text{B}+10\%\text{Fe}$ nanocomposite milled between 4 and 12 h and annealed for the indicated conditions. The magnetic hysteresis loops for hard magnetic phase milled and annealed in the same conditions is presented for comparison.

improvement of the coercivity of the samples milled for short milling times. The evolution of magnetic hysteresis loops for the sample of hard magnetic phase, $\text{Nd}_2\text{Fe}_{14}\text{B}$ milled for 2 h and annealed at 550 °C for 1.5 h compared with the evolution of the hysteresis loops for 4 h nanocomposite annealed in the same conditions can be explained by the new microstructure given by the presence of Fe and possible secondary phase Fe_3B [95, 98, 99].

The magnetic behaviour of $\text{Nd}_2\text{Fe}_{14}\text{B}+10\% \text{Fe}$ magnetic nanocomposite obtained by mechanical milling and subsequently short heat treatment has been studied from magnetic hysteresis loops measurements and dM/dH vs. H curves [98]. The demagnetization curves for $\text{Nd}_2\text{Fe}_{14}\text{B}+10\% \text{Fe}$ composite milled for 8 h and annealed at 700 and 750 °C for different times are plotted in figure 5.7 (8 h MM + 700 °C/x minutes) and figure 5.8. (8 h MM + 750 °C/x minutes). The demagnetization curves for 8 h milled magnetic nanocomposite sample and 8h milled and annealed at 550 °C for 1.5h nanocomposite sample are given for comparison. For all samples we have applied the correction for demagnetization field, considering spherical shapes samples the demagnetization factor is 1/3. The saturation behaviour of the samples is illustrated in the inset of both figures. From both figures we can observe an obvious improving of the coercivity and remanence after annealing, either conventional or rapid annealing. The coercivity of samples obtained by rapid annealing is higher than the coercivity of the samples obtained by classical annealing. On the contrary, the

remanence magnetization is slightly larger for the sample obtained by conventional annealing. This behaviour could be connected with the decrease of the exchange strength of α -Fe, given by the slight increase of Fe crystallites.

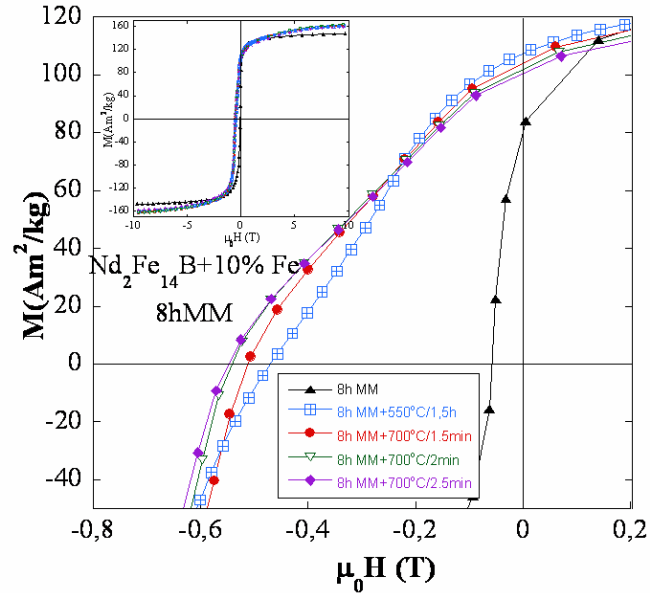


Figure 5.7. Demagnetization curves recorded for $\text{Nd}_2\text{Fe}_{14}\text{B}+10\% \text{Fe}$ composite milled 8 h, as-milled sample and annealed sample at 550 and 700 °C for time indicated in figure. The corresponding hysteresis curves are given in inset.

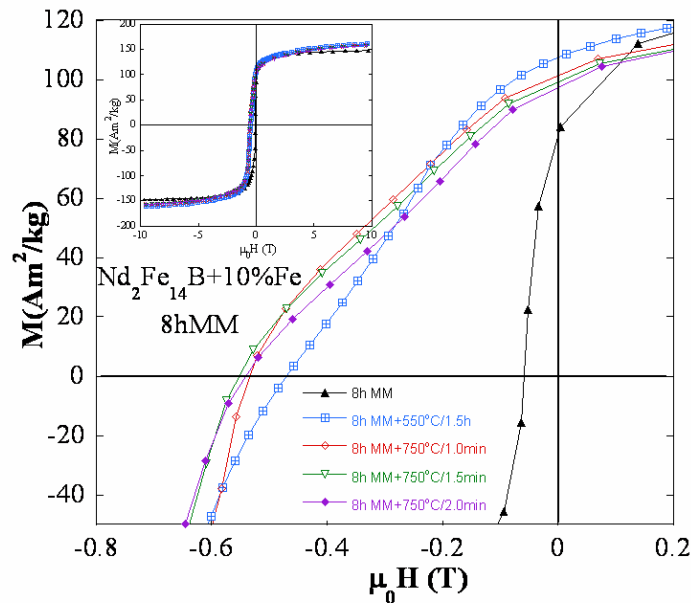


Figure 5.8. Demagnetization curves recorded for $\text{Nd}_2\text{Fe}_{14}\text{B}+10\% \text{Fe}$ composite milled 8 h, as-milled sample and annealed sample at 550 and 750 °C for time indicated in figure. The corresponding hysteresis curves are given in inset.

The evolution of the coercive field vs. annealing conditions is illustrated in figure 5.9. By this preparation method, after 8 h of dry milling and different heat treatments, a maximum coercivity of 0.59 T can be reached. The importance of annealing time and temperature is well illustrated in figure 5.9. Comparable coercivity of magnetic nanocomposite can be attained for short annealing time when increasing the annealing temperature.

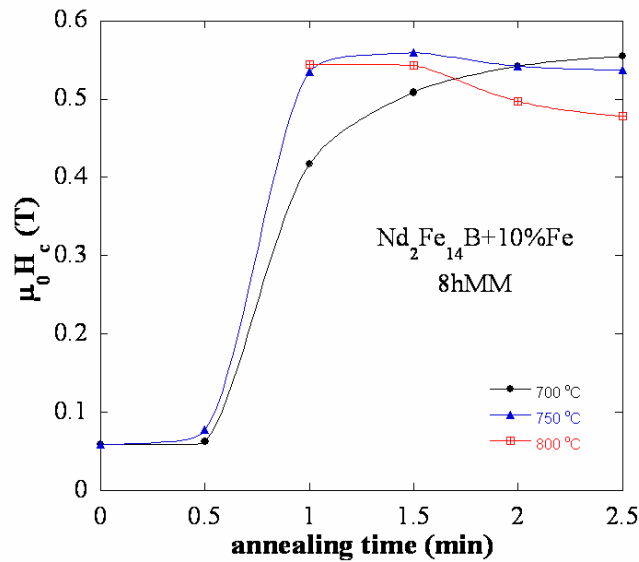


Figure 5.9. Coercive fields vs. annealing for $\text{Nd}_2\text{Fe}_{14}\text{B}+10\%\text{Fe}$ composite milled 8 h and annealed at 700, 750 and 800 °C

5.3. Study of magnetic behaviour and exchange coupling of $\text{R}_2\text{Fe}_{14}\text{B} + 22 \text{ wt}\% \alpha\text{-Fe}$ ($\text{R} = \text{Nd}, \text{Nd}+\text{Dy}$) magnetic nanocomposite

The evolution of coercivity and magnetisation of $(\text{Nd}_{0.92}\text{Dy}_{0.08})_2\text{Fe}_{14}\text{B} + 22 \text{ \% Fe}$ nanocomposite samples as milled and milled and annealed was studied by measuring the hysteresis loops and from dM/dH vs. H curves. The value of coercive fields vs. annealing time are illustrated in figure 5.10. The $(\text{Nd}_{0.92}\text{Dy}_{0.08})_2\text{Fe}_{14}\text{B} + 22 \text{ \% Fe}$ magnetic nanocomposite milled between 4 and 12 hours shows a linear decrease of the coercive field value with increasing milling time.

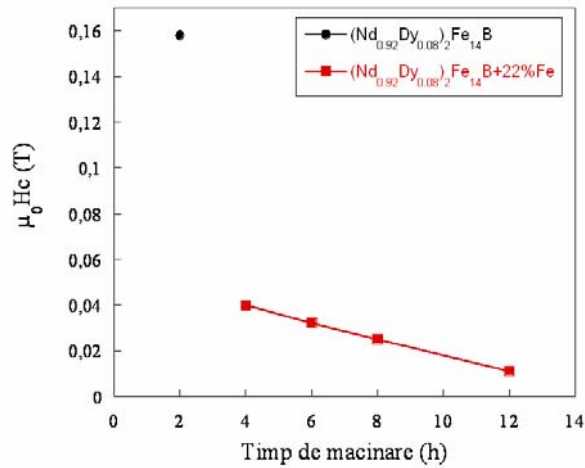


Figure 5.10. Coercive field evolution vs. annealing time for $(Nd_{0.92}Dy_{0.08})_2Fe_{14}B + 22\%$ milled between 4 and 12 hours and for $(Nd_{0.92}Dy_{0.08})_2Fe_{14}B$ milled for 2 hours.

The recovery of crystal structure by annealing leads to increased nanocomposite coercivity. As we presented, the hard/soft coupling is better evidenced from the study of $dM/dH = f(H)$ curves. For that purpose, in figure 5.11 were plotted dM/dH vs. magnetic field curves for the samples annealed at 550 °C (figure 5.11 a), 600 °C (figure 5.11 b) and 800 °C (figure 5.11 c). The peak which occurs at low field, in all the cases, correspond to the non coupled hard and soft magnetic phases, while the maximum which occurs at higher values of the field corresponds to the hard/soft coupled composite. Studying the evolution of the peaks at small magnetic fields (from figure 5.11) we see a slight increase of that for samples annealing at 600 °C and a net increase up to the characteristic peak of coupled composite for the sample annealed at 800 °C for 5 minutes.

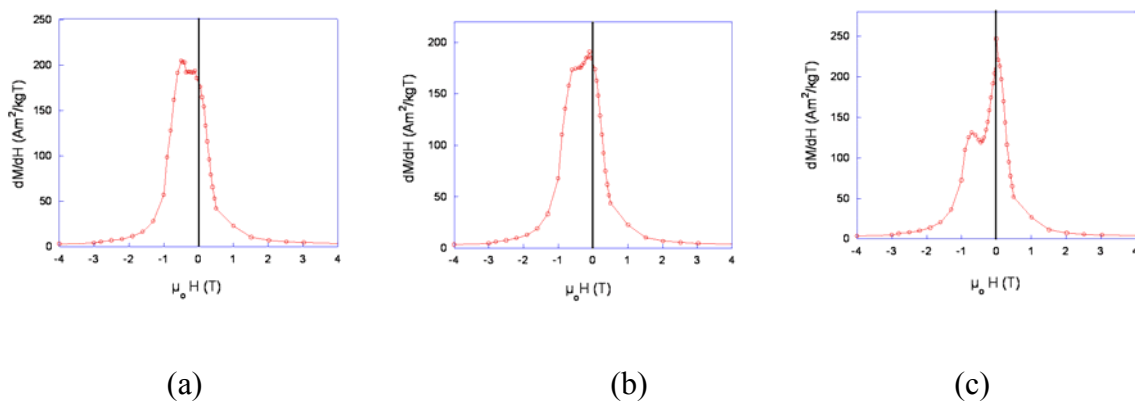


Figure 5.11 dM/dH vs H curves of $(Nd_{0.92}Dy_{0.08})_2Fe_{14}B + 22\%$ Fe composite milled for 6 hours and annealed for 1.5 hour at 550 °C (a), 600 °C (b) and annealed for 5 minutes at 800 °C (c)

The values of coercive field and remanent magnetisation of $(\text{Nd}_{0.92}\text{Dy}_{0.08})_2\text{Fe}_{14}\text{B} + 22\%$ Fe magnetic nanocomposite samples milled for 8 h and annealed at 550 °C for 14 h and for $\text{Nd}_2\text{Fe}_{14}\text{B} + 22\%$ Fe nanocomposite milled 8 h and annealed at 700, 750 and 800 °C for times between 0.5 and 2.5 minutes are presented in table 5.3. We remark, that for classical heat treatment even if an amount of Nd was substituted with Dy for enhancement the coercivity, the coercive field values are significantly lower than those obtained in the nanocomposite annealed for short times. SHT lead to values of coercive fields and remanent magnetization improved in comparison with values obtained for classical annealed samples. From study of crystallographic and magnetic measurements results we find that the better magnetic properties for $\text{Nd}_2\text{Fe}_{14}\text{B} + 22\%$ Fe is: annealing temperature 700, 750 and 800 °C for annealing time of 1.5 – 2.5 min, 1.5 – 2 min and 1 min respectively.

Table 5.4. Coercive field and remanent magnetization for $(\text{Nd}_{0.92}\text{Dy}_{0.08})_2\text{Fe}_{14}\text{B} + 22\%$ Fe nanocomposite obtained after 8 h of milling and annealed at 550 °C and for $\text{Nd}_2\text{Fe}_{14}\text{B} + 22\%$ Fe nanocomposite milled for 8 h and annealed at 700, 750 and 800 °C for indicated times. The sample marked with * is treated for 14 hours

Temperatura de tratament termic (°)	Timpul de tratament termic (min)	$\mu_0 H_c$ (T)	M_r (Am^2/kg)
700	0.5	0.05	16.14
	1	0.26	51.72
	1.5	0.33	56.31
	2	0.33	55.31
	2.5	0.30	57.30
750	0.5	0.06	19.43
	1	0.32	56.31
	1.5	0.32	56.60
	2	0.32	56.60
	2.5	0.30	52.32
800	0.5	0.06	19.43
	1	0.34	55.39
	1.5	0.28	47.72
	2	0.28	47.72
	2.5	0.26	46.34
550	14 h*	0.18	46.15
0	0	0.02	10.74

The evolution of coercive field vs. annealing time for SHT is illustrated in figure 5.12. The coercive field has a strong growth after the first minute of annealed for all the annealed temperatures considered in this study. For 30 second of annealing there is a slightly raising sloop in comparison with the sloop for 1 minute. This behaviour can be attributed to the fact that after 30 seconds the temperature is not enough homogenized in the mass of the sample and the time is not long enough to have an efficiently diffusion of elements to obtained an

reconstruction of hard magnetic phase. Instead, after 1 and 2 minutes of annealing we see a saturation process in the increasing phase. After reaching the limit of this increase of the coercivity is appeared a descendent slope in the dependence of coercivity vs. annealing time, for long annealing times. This behaviour is attributed to recrystallization processes and to an increasing of crystallites of hard magnetic phase.

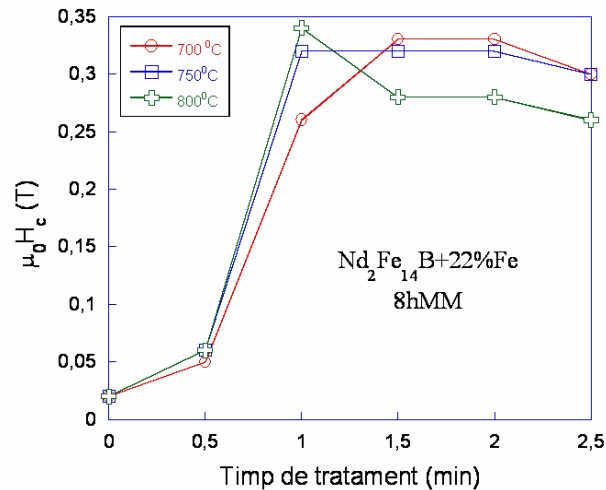


Figure 5.12 Coercive field values vs annealing for Nd₂Fe₁₄B+22%Fe composite annealed for 8 hours and annealed at 700, 750 and 800 °C. The first value of coercive field belongs to the composite substituted with Dy.

5.6. Conclusions

The R₂Fe₁₄B + x wt % α-Fe (where R = Nd or Nd+Dy and x = 10 or 22) type nanocomposite were obtained by mechanical milling method. After milling were performed two different annealing: a short HT (Nd₂Fe₁₄B + x wt % Fe; where x = 10 or 22) and a long HT (Nd₂Fe₁₄B + x wt % Fe, where R = Nd or Nd + Dy, and x = 10, 22). For all the sets of samples, the milling leads to a decrease of crystallite size dimensions, increase the density of defects and occurrence to the internal stress. By increasing the milling time, the value of coercive field decrease drastically due to the amorphisation of crystal structure of hard magnetic phase. The annealing performed lead to a decrease of density of defects reduces the internal stress and restores the crystallinity of phases of magnetic composite. For both sets of sample classical annealed, the optimal annealing temperature is about 550 °C. In the case of SHT, the best magnetic properties, μ₀H_c=0,34 T, were obtained for samples annealed at temperature of 700, 750 and 800 °C for 1.5 – 2.5 min, 1,5 – 2 min and 1 min respectively. The

strength of the exchange coupling between hard magnetic phase and soft magnetic phase can be improved by adjusting the amount of soft magnetic phase and for a given iron content by changing the milling conditions and annealing conditions.

General conclusions and perspectives

The purpose of this paper is the study of structure, microstructure, and magnetic behaviour of magnetic materials such as hard/soft exchange coupled materials. The structural and microstructural measurement results were correlated with magnetic measurement results. The studied magnetic materials were obtained by mechanical milling and subsequently annealed. It was obtained and studied hard magnetic phase, $\text{Nd}_2\text{Fe}_{14}\text{B}$, soft magnetic phase, α -Fe and four sets of $\text{R}_2\text{Fe}_{14}\text{B} + x \text{ wt } \% \alpha - \text{Fe}$ (where $\text{R} = \text{Nd}$ or $\text{Nd} + \text{Dy}$ and $x = 10$ or 22) nanocomposite type.

Following the milling process, for all the samples is found an increase of defects, induced internal stress, decrease of the crystallites size and a destruction of crystal structure. These effects lead to large diffractions peaks of both samples. As milling time increase, the effects mentioned above are more pronounced, the crystallinity of samples decreased with increasing the milling time. The reduce of the crystallite size is achieved when numerous processes of fission and fragmentation occur. The milling effect is more pronounced for hard magnetic phase than in the soft magnetic phase.

One of the requirements in order to achieve the exchange coupling is given by the large as possible magnetic anisotropy. These requirements may be accomplished by performing the annealing for recrystallisation of hard magnetic phase but in the same time the annealing should not lead to an increase of the size of crystallites higher than double of domain wall of hard magnetic phase. In order to establish the optimum annealing conditions were performed DSC measurements. Based on the analysis of DSC curves we established two types of annealing, classical heat treatment, CHT done for the times to 14 hours and short heat treatment done for times up to 3 minutes. The annealing lead to lower density of defects, reduced internal stress, has rearranged the atoms in structure and similar possible effects of recrystallisation.

In order to establish the optimum milling and annealing conditions the paper propose an individual study of hard phase, $\text{Nd}_2\text{Fe}_{14}\text{B}$ and soft phase, Fe. The optimum annealing temperature for CHT is $550 \text{ }^\circ\text{C}$ for 2 hours and for SHT is $800 \text{ }^\circ\text{C}$ for 1 minute. By applying this annealing we have succeeded to recover the crystallinity of hard magnetic phase without leading to an increase of crystallites size of soft magnetic phase up to the limit of optimum exchange coupling. By comparing the degree of crystallinity of hard magnetic phase we concluded that the best crystallinity of hard magnetic phase is obtained after the performing SHT. At the same time diffraction peaks of the soft magnetic phase obtained by the two

methods of annealing have comparable Full-Width- at Half-Maximum. In the case of SHT, both time and temperature are critical parameters in obtaining desired crystallographic and magnetic properties while in the case of CHT annealing temperature parameter is essential in archiving the final properties of the sample.

In the structural evolution of the composite we meet similar effects to those found for hard and soft magnetic phases studied separately. By annealing we have succeeded to improve the crystallinity of samples affected by grinding, and this has led to increase of hard/soft coupling. Optimum annealing temperature for CHT is 550 °C. In the case of the composite annealed for a short period of time the optimum conditions are: 700, 750 and 800 °C for 1.5 – 2.5 min, 1.5 -2.5 min and 1 min respectively. SHT lead to crystallographic and magnetic properties greatly improved in comparison with CHT, the coercive fields are higher by 20 %.

One of the conclusions of the presented study points out that the destruction by milling of crystal structure of hard magnetic phase affects hard/soft interphase exchange coupling. Crystallographic recovery of hard magnetic phase by annealing is limited by the tendency of growth of soft magnetic phase crystallite. Therefore, a direction for the future studies is to preserve the partial crystallinity of hard magnetic phases by reducing the milling time. Another issue considered refers to the reduction of interphase diffusion during milling and annealing. One way concerning this is to perform the wet milling of composite in the presence of a surfactant. The composite microstructure can be improved by optimizing the milling and annealing conditions.

Selected references

6. E. Burzo, '*Magneti permanenti*' vol. 1, Ed. Acad. Rep. Socialiste Roamnia, Bucuresti, 1986.
11. F. Kneller, R. Haing, IEEE Trans. Magn. 27 (1991) 3588.
12. V. Pop Proceedings of Remanian – France School, magnetisme des systemes nanoscopiques et structures hybrids Brasov 1 – 10 september 200. ISBN 973-647-176-6, p VI. 1-12
13. K.H.J. Buschow, Handbook of Mag. Mater., Ed. K. H. J. Buschow, 10° (1997) 463.
14. R. Coehoorn, D. B. de Mooij, C De Waard, J. Mag. Magn. Mater, 80° (1989) 101.
15. R Skomski, J. Phys, ° Condens matter 15 R (2003) 841.
16. R. Skomski, J. M. Coey, Permanent Magnetism, 1999 (Bristol : Institute of Physics Publishing).
17. G. C. Hadjipanays, J. Mag. Magn. Mater 200° (1999) 373.
18. Z. D. Zhang, W. Liu, J. P. Liu, D. J. Sellmayer, J. Phys. D, Appl. Phys. R217, (2000) 330.
19. Roskilde, J. Petrold, J. Magn. Magn. Mater 84 (2002) 242-245.
20. T. Schrefl, J. Fidler, H. Kromuller, Phys. Rev. B 49 (1994) 6100.
33. E. Dorolti, V.Pop, O. Isnard, D. Givord, I. Chicinas, J. Opt. Adv. Mater. 9 (2007) 1471-1477.
36. O. Gutfleisch, A. Bollero, A. Handstein, D. Hinz, A. Kirchner, A. Yan, K. H. Muller, L Schultz, J. Magn. Magn. Mater 242-245 (2002) 1277.
41. L. Schultz, K. Schnitzke, J. Wecker, M. Katter, C. Kuhrt, J. Appl. Phys. 70 (1991) 6339.
42. K. O'Donnell, J. M. D. Coey, J. Appl. Phys 81 (1997) 6311.
43. L. Wei, W Qun, X. K. Sun, Z. Xin-guo, Z. Tong, Z. Zhi-dong, Y. C. Chuang, J. Magn. Magn. Mater 131 (1994) 413.
44. J. X. Zhang, L. Bessais, C. Djega-Maraiadassou, E. Leroy, A. Percheron-Guegan, Y. Champion, Appl. Phys. Lett 80 (2002) 1960.
45. D. L. Leslie-Pelecky, R. L. Schalek, Phys. Rev. B59 (1999) 457.
46. D. Geng, Z. Zhang, B. Cui, Z. Guo, W. Liu, X. Zhao, T. Zhao, J. Liu, J. Alloy and Compounds 291 (1999) 276.
47. C. You, X. K. Sun, W Liu, B. Cui, X. Zhao, ZZhang, J. Phys. D. Appl Phys. 33 (2000) 926

48. W. Liu, Z. D. Zhang, J. P. Liu, X. K. Sun, D. J. Sellmyer, X. G. Shao, J. Magn. Magn. Mater 221 (2000) 278.
49. R. Grossinger Reiko Sato, J. Magn. Magn. Mater. 294 (2005) 91.
50. M. A. Al-Khafaji, W. M. Rainforth, M. R. Gibbs, H. A. Dovies, J E L Bishop, J. Magn. Magn. Mater 188 (1998) 109
51. A. Bollero, A. Yan, O. Gutfleisch, K. H. Muller, L. Schultz, IEEE Trans Magn 39 (2003) 2944.
52. V. Pop O. Isnard, I. Chicinas, D. Givord, J. M. Le Breton, J. Optoelectron Adv. Mater. 8 (2006) 494.
53. V. Pop, O. Isnard, I. Chicinas, D. Givord, J. magn. Magn. Mater 310 (2007) 2489.
54. V. Pop, I. Chicinas, J. Optoelectron, Adv. Mater. 9 (2007) 1478.
55. D. Givord, O. Isnard, V. Pop, I. Chicinas, J. Magn. Magn. Mater. 316 (2007) e 503.
94. Scherrer Göt. Nachr. 2 (1918) 98.
95. O. Isnard, D. Givord, E. Dorolți, V. Pop, L. Nistor, A. Tunyagi, I. Chicinaș, J. Optoelectron, Adv. Mater. 10 (2008) 1819-1822.
96. S. Guțoiu, E. Dorolți, O. Isnard, V. Pop, J. Optoelectron, Adv. Mater. 12 (2010) 2126-2131.
97. S. Guțoiu, Al. Trifu, O. Isnard, M. Văleanu, F. Popa, I. Chicinaș, V. Pop, E. Dorolți Buletinul Inst. Politehnic din Iași, Tomul LVII (LXI), Fasc. 2, 2011.
98. V. Pop, S. Guțoiu, E Dorolți, O. Isnard, I. Chicinaș, J. Alloy and Compounds 509 (2011) 9964.
99. Shandong Li, et al. J. Magn. Magn. Mater. 282 (2004) 202-205.
104. S. Gutoiu, E. Dorolti, O. Isnard, I. Chicinas, V. Pop, Proc. Materiaux 2010 Congrès, Nantes, France, (2010).
106. R. Skomski, J. Appl. Phys. 76 (1994) 7059.
107. S. Gutoiu, E. Dorolti, O. Isnard, I. Chicinaș, F. Popa, V. Pop, World Powder Metallurgy Congress@Exhibition, PM 2010, oct. 2010, Florence, Proceedings, vol. V, 271-276.

Some of the research presented in this thesis have been published in scientific journals or presented at scientific conferences or international summer schools:

1. V. Pop, **S. Guțoiu**, E. Dorolți, O. Isnard, I. Chicinaș,
The influence of short time heat treatment on the structural and magnetic behaviour of Nd₂Fe₁₄B/ α Fe nanocomposite obtained by mechanical milling
Journal of Alloys and Compounds 509 (2011) 9964-9969
2. **S. Guțoiu**, Al. Trifu, O. Isnard, M. Văleanu, F. Popa, I. Chicinaș, V. Pop, E. Dorolți
Microstructure studies of milled hard and soft magnetic phases for exchange coupled Nanocomposite
Buletinul Institutului Politehnic din Iași Tomul LVII (LXI), Fasc. 2 , 2011
3. **S. Guțoiu**, E. Dorolți, O. Isnard, I. Chicinaș, V. Pop
Magnetic and structural behaviour of Nd₂Fe₁₄B/α-Fe and (NdDy)₂Fe₁₄B/α-Fe obtained by mechanical milling and annealing
J. Optoelectron. Adv. Mater. 12 (2010) 2126-2131
4. O. Isnard, V. Pop, E. Dorolți, **S. M. Guțoiu**, A. Takacs, I. Chicinaș
Microstructure Evolution of (Pr,Dy)₂Fe₁₄B/αFe Nanocomposite Coupled by Exchange Interactions.
Studia Univ. “Babeș-Bolyai”, Physica, 55, no. 1 (2010) 63-71

Summer schools and conferences participation

1. E. Dorolți, **S Guțoiu**, O Isnard, I Chicinas, V. Pop
The influence of short time heat treatment on the structural and magnetic behaviour of Nd₂Fe₁₄B/ α-Fe nanocomposite obtained by mechanical milling
Euromat 2011 Montpellier
2. **S. Guțoiu**, M. Valeanu, E. Dorolți, O. Isnard, I. Chicinas, V. Pop
The influence of the annealing conditions on the crystallite size of Nd₂Fe₁₄B/α-Fe nanocomposites obtained by mechanical milling
JEMS 2010, 23-28 aug. Cracovia.

3. **S. Gutoiu**, E. Dorolti, O. Isnard, M. Valeanu, I. Chicinas, V. Pop
Microstructure Studies of Milled Hard and Soft Magnetic Phases for Nd₂Fe₁₄B/ α -Fe Nanocomposite
International Balkan Workshop on Applied Physics, IBWAP-2010 Constanta 7-9 July 2010
4. **S. Gutoiu**, A. Trifu, E. Dorolti, O. Isnard, M. Valeanu, F. Popa, I. Chicinas, V. Pop
Microstructure Studies of Milled Hard and Soft Magnetic Phases for Exchange Coupled Nanocomposite
National Conference of Applied Physics Iași 2010
5. **S. Gutoiu**, E. Dorolti, O. Isnard, I. Chicinas, F. Popa, V. Pop
Magnetic and Structural Behaviour of Nd₂Fe₁₄B/ α -Fe Magnetic Nanocomposite
World Powder Metallurgy Congress@Exhibition, PM 2010, oct. 2010, Florence, Proceedings, vol. V, 271-276 Powder Metallurgy Conference Florenta 2010
6. **S. Gutoiu**, E. Dorolti, O. Isnard, I. Chicinas, V. Pop
Elaboration d'aimants nanocomposites R₂Fe₁₄B/ α -Fe (R=Nd, Dy) par broyage mécanique, caractérisation de leurs propriétés structurales et magnétiques
Materiaux 2010 Congrès, Nantes, France, 18-22 Oct. 2010
7. **S. Guțoiu**, E. Dorolți, O. Isnard, I. Chicinaș, T. Nemțanu, V. Pop
Structural and magnetic behaviour of Nd₂Fe₁₄B/ α -Fe nanocomposites obtained by mechanical milling and subsequent annealing
European School on Magnetism, Timișoara, România, 2009